Eur. Phys. J. B (2017) 90: 255
DOI: 10.1140/epjb/e2017-80563-y

THE EUROPEAN PHYSICAL JOURNAL B

Regular Article

Entanglement generation through the interplay of harmonic driving and interaction in coupled superconducting qubits

Ana Laura Gramajo, Daniel Domínguez, and María José Sánchez[a]

Centro Atómico Bariloche and Instituto Balseiro, 8400 San Carlos de Bariloche, Argentina

Received 3 August 2017 / Received in final form 6 October 2017
Published online 18 December 2017 – © EDP Sciences, Società Italiana di Fisica, Springer-Verlag 2017

Abstract. We study the manipulation of quantum entanglement by periodic external fields. As an entanglement measure we compute numerically the concurrence of two coupled superconducting qubits both driven by a dc + ac external control parameter. We show that when the driving term of the Hamiltonian commutes with the qubit–qubit interaction term, it is possible to create or destroy entanglement in a controlled way by tuning the system at or near multiphoton resonances. On the other hand, when the driving does not commute with the qubit–qubit interaction, the control and generation of entanglement induced by the driving field is more robust and extended in parameter space, beyond the multiphoton resonances.

1 Introduction

The control and manipulation of entanglement is one of the central prerequisites of quantum computing architectures in order to exploit the non local quantum correlations. Today, entanglement has been demonstrated in a large variety of physical systems like ultracold atomic ensembles [1,2], ion traps [3,4] and cavity quantum electrodynamics devices based on superconducting qubits [5–8]. Among these, solid state superconducting circuits based on Josephson junctions are promising due to their microfabrication techniques and downscalability [9–13]. In these devices, the generation and control of entanglement have been tested under various schemes [14–17]. For instance, pulse sequences have been implemented for several superconducting qubits with fixed interaction energies [18,19], and tunable coupling schemes have been proposed [13,20–22]. Alternatively, engineering selection rules of transitions among different energy levels is a possible strategy for coupling and decoupling superconducting qubits [23,24].

The sensitivity of the energy levels of superconducting qubits driven by an external magnetic flux (ac + dc) has been extensively studied in recent years [25–31]. Microwave fields has become a tool to analize quantum coherence and to access the multilevel structure of these artificial atoms under strong driving [32–37].

Profiting from these ideas, in this work we study the manipulation of entanglement between two superconducting qubits by external driving fields of variable amplitude and fixed frequency. In particular we analyze how the strength and the kind of coupling between the two qubits affect the dynamics and the entanglement, considering different static couplings for a given microwave driving field configuration. Entanglement generation in ac-driven systems has been amply investigated in the literature, but mostly in the case of one and two photon resonances and for low ac amplitudes. Here we will investigate entanglement control and generation near multiphoton resonances and for large ac amplitudes, in the context of Landau–Zener–Stuckelberg interferometry [26,32–34,36,37].

The system of work consists in two coupled superconducting qubits driven by (the same) microwave field. As usual, each qubit is represented by a two level system [38–40] and we focus here on qubits with large decoherence times such that the effects of dissipation and/or interaction with the environment are negligible. For flux qubits [9,32], the natural interaction is between the magnetic fluxes, providing a coupling through their mutual inductance [9,17,32]. On the other hand, for phase or charge qubits the dominant coupling is essentially capacitive [13,19,41].

As a measure of entanglement we choose the *concurrence* [42] which vanishes for non entangled states and reaches its maximum value 1, for maximally entangled states. Using state tomography, in reference [43] the full density matrix of a two qubit system has been measured and the concurrence and the fidelity of the generated state determined, providing an experimental proof of entanglement. Recently, the ability to perform time-continuous measurements has enabled to observe the dynamics of the emergence of entanglement for two qubits separated by macroscopic distances [44,45]. Additionally there are other proposals based on the measurement of the ground state population of two copies of a bipartite system [46], that could give direct access to the concurrence for pure states.

In this work we calculate the concurrence in terms of Floquet states and quasienergies, providing an analytical expression for a lower bound of the concurrence.

[a] e-mail: majo@cab.cnea.gov.ar

We take into account different types of coupling between the two qubits, longitudinal (i.e. commuting) and transverse (non-commuting) with respect to the driving term, and study the dependence of the concurrence on the parameters of the microwave field and the coupling strengths. We analyse the conditions for control and generation of entanglement, finding very different behaviours mainly determined by the commutability of the driving term with the qubit–qubit interaction.

2 Concurrence for the two coupled qubits model

The dynamics of two coupled superconducting qubits can be described by the global Hamiltonian [13]

$$\hat{H} = -\frac{1}{2}\sum_{i=1}^{2}\left(\epsilon_i\sigma_z^{(i)} + \Delta_i\sigma_x^{(i)}\right) + \hat{H}_{12} + V(t), \qquad (1)$$

where ϵ_i is the detuning energy (which can be controlled with a magnetic flux in the case of flux qubits, or with gate voltages in the case of charge qubits), Δ_i is the tunnel splitting energy and $\sigma_z^{(i)}, \sigma_x^{(i)}$ the Pauli matrices, with $i = 1, 2$ the index of each qubit. $\hat{H}_{12}$ is the coupling Hamiltonian, which in general can be written as:

$$\hat{H}_{12} = -\frac{J^z}{2}\sigma_z^{(1)}\sigma_z^{(2)} - \frac{J^c}{2}\left((1-p)\sigma_x^{(1)}\sigma_x^{(2)} + p\sigma_y^{(1)}\sigma_y^{(2)}\right), \qquad (2)$$

with J^z and J^c the correspondent coupling constants. Different physical coupling schemes between superconducting qubits are represented by this Hamiltonian. For example, the case $J^c = 0$ and $J^z \neq 0$ corresponds to flux qubits with inductive coupling [17] and charge qubits with capacitive coupling; the case $J^z = 0$, $J^c \neq 0$, $p = 0.5$ corresponds to charge qubits connected via a Josephson junction and to phase qubits with a capacitive coupling, $J^z = 0$, $J^c \neq 0$, $p = 1$ corresponds to charge qubits connected through a common LC oscillator; $J^z = 0$, $J^c \neq 0$, $p = 0$ corresponds to charge-phase qubits coupled by connecting loops with a Josephson junction in the common link, etc. (see for example [13] for a review).

In the presence of driving fields we have the term [47]

$$V(t) = -\frac{1}{2}\sum_{i=1}^{2} v_i(t)\sigma_z^{(i)}, \qquad (3)$$

where $v_i(t) = A_i\cos(\omega t - \varphi_0)$ is the driving microwave field of amplitude A_i and frequency ω applied to each qubit.

The resulting Hamiltonian is thus periodic in time, $\hat{H}(t) = \hat{H}(t+T)$ with period $T = 2\pi/\omega$. According to the Floquet theorem [35,38,39], the solution of the Schrödinger equation can be spanned in the Floquet basis $\{|u_\alpha(t)\rangle\}$ as $|\Psi(t)\rangle = \sum_\alpha a_\alpha(t_0)e^{-i\gamma_\alpha t/\hbar}|u_\alpha(t)\rangle$, with γ_α the quasienergies and α the index labeling the eigenstates of the time independent problem. For an initial condition $|\Psi(t_0)\rangle$ at time t_0, we define the coefficients $a_\alpha(t_0) = \langle u_\alpha(t_0)|\Psi(t_0)\rangle$. The time-evolution for Floquet states is given by $(H(t) - i\hbar\frac{\partial}{\partial t})|u_\alpha(t)\rangle = \gamma_\alpha|u_\alpha(t)\rangle$, and they satisfy $|u_\alpha(t+T)\rangle = |u_\alpha(t)\rangle$. Therefore after expanding the time periodic Floquet states in the Fourier basis, $|u_\alpha(t)\rangle = \sum_k e^{ik\omega t}|u_\alpha(k)\rangle$ the time-dependent problem is reduced to a time-independent eigenvalue problem.

An entanglement measure quantifies the degree of quantum correlations present in a given quantum state. In the case of pure states $|\Psi(t)\rangle$ a useful quantity is the concurrence [42],

$$C(t,t_0) = |\langle\Psi(t)|^*\sigma_y^{(1)}\otimes\sigma_y^{(2)}|\Psi(t)\rangle|, \qquad (4)$$

that goes from 0 for non-entangled states, to 1 for maximally entangled states. Notice that equation (4) depends implicitly on the initial time t_0 through $|\Psi(t)\rangle$.

Using the extended Floquet basis in Fourier space $\{|u_\alpha(k)\rangle\}$ with $k \in \mathbb{Z}$, equation (4) can be written as

$$C(t,t_0) = |\sum_{\alpha\beta kk'qq'}\tilde{C}_{\alpha\beta}(k,k') \times f_{\alpha\beta}(q,q')e^{-i\varphi_{\alpha\beta}^{kk'qq'}(t,t_0)}|, \qquad (5)$$

where $\varphi_{\alpha\beta}^{kk'qq'}(t,t_0) = (\gamma_\beta + \gamma_\alpha - (k'+k)\omega)t - (\gamma_\beta + \gamma_\alpha - (q'+q)\omega)t_0$, with γ_β^α the quasienergies, $\tilde{C}_{\alpha\beta}(k,k') = \langle u_\alpha(k)|^*\sigma_y^{(1)}\otimes\sigma_y^{(2)}|u_\beta(k')\rangle$ and $f_{\alpha\beta}(q,q') = a_\alpha(q)a_\beta(q')$, with $a_\beta^\alpha(q') = \langle u_\beta^\alpha(q')|\Psi(t_0)\rangle$ (see Appendix A). It is useful to characterize the typical concurrence of a time dependent system with the average:

$$\overline{\overline{C}} = \lim_{t'\to\infty}\frac{1}{t'}\int_0^{t'}dt\,\frac{1}{T}\int_0^T dt_0\,C(t,t_0). \qquad (6)$$

The average over initial time t_0 corresponds to an average over an unknown initial phase $\varphi_0 = \omega t_0$ of the microwave fields $v_i(t) = A_i\cos(\omega t - \varphi_0)$, while the average over t gives a typical value of the concurrence through the duration of the drive.

3 Results

To solve the dynamics we compute numerically the Floquet states and quasienergies, and we calculate the concurrence using equation (5) with the averages over t_0 and t given in equation (6). Along this work, we fix $\epsilon_i = \epsilon_0$, $\forall i = 1, 2$, and choose $\Delta_1/\omega = 0.1$ and $\Delta_2/\omega = 0.15$. We take $\hbar = 1$ and energy scales are normalized by ω.

The main ingredient in the discussion of our results will be the commutator between the driving $V(t)$ and the qubit–qubit coupling term:

$$[V(t),\hat{H}_{12}] = i\frac{J^c(v_1+v_2)(1-2p)}{4}\left(\sigma_y^{(1)}\sigma_x^{(2)} + \sigma_x^{(1)}\sigma_y^{(2)}\right) + i\frac{J^c(v_1-v_2)}{4}\left(\sigma_y^{(1)}\sigma_x^{(2)} - \sigma_x^{(1)}\sigma_y^{(2)}\right). \qquad (7)$$

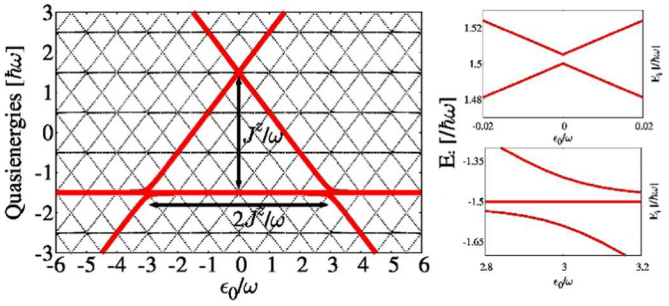

Fig. 1. Eigenenergies E_i in the absence of driving, $A/\omega = 0$ (red lines) and quasienergies for $A/\omega = 3.8$ (black lines) as a function of ϵ_0/ω, for the coupling strength $J^z/\omega = -3$. Parameters are $\Delta_1/\omega = 0.1$ and $\Delta_2/\omega = 0.15$. The two panels at the right show enhanced plots of avoided crossings of the eigenenergies.

We will call "longitudinal coupling" the case when the coupling commutes with the driving term (when $J^c = 0$), and "transverse coupling" the case when the coupling does not commute with the driving term (when $J^c \neq 0$). To further simplify the analysis we will consider here the same driving in both qubits $v_1(t) = v_2(t)$, in which case $[V(t), \hat{H}_{12}] \propto J^c(1-2p)$.

3.1 Longitudinal coupling

We start with the results for the "longitudinal coupling" case, with $J^z \neq 0$ and $J^c = 0$, for which driving and coupling commute: $[V(t), \hat{H}_{12}] = 0$. This is the situation typically realized in flux qubits, where the qubit–qubit coupling is inductive and the driving is through a time dependent magnetic flux [17,47].

Figure 1 shows as a function of the detuning ϵ_0/ω and $J^z/\omega = -3$, the eigenenergies E_i, $i = 0, \ldots, 3$ for the time independent Hamiltonian (red lines), and in black the quasienergies for the driven Hamiltonian for $A/\omega = 3.8$. We work with the (antiferromagnetic) coupling $J^z < 0$, which reduces the energy of states $|01\rangle, |10\rangle$ while it increases the energy of states $|00\rangle, |11\rangle$, with $\mathcal{E} = \{|00\rangle, |01\rangle, |10\rangle, |11\rangle\}$ the computational basis in the product space of the two qubits.

The quasienergies display avoided crossings (quasidegeneracies), where the Floquet states are strongly mixed. These quasidegeneracies will play a central role in the structure of the concurrence as we will discuss in the following.

For the present case of longitudinal coupling, the quasienergies of the two qubit system can be computed analytically in the limit $\Delta_i/\omega \to 0$ using the Van Vleck nearly degenerate perturbation theory [38]. We obtain $\gamma_\alpha \sim \pm\epsilon_0 + J^z/2 + m\omega$ and the (quasi) degenerate pair $-J^z/2 + m\omega$ with $m \in \mathbb{Z}$. As the driving $V(t)$ and the static coupling Hamiltonian are both proportional to σ_z, the location of the quasi crossings in the spectrum of quasienergies are replicas (in $\pm m\omega$) of the quasi crossings of the static spectrum (see Fig. 1). The resonance conditions, $\gamma_\alpha - \gamma_\beta = n\omega$ ($n \in \mathbb{Z}$), are thus satisfied respectively

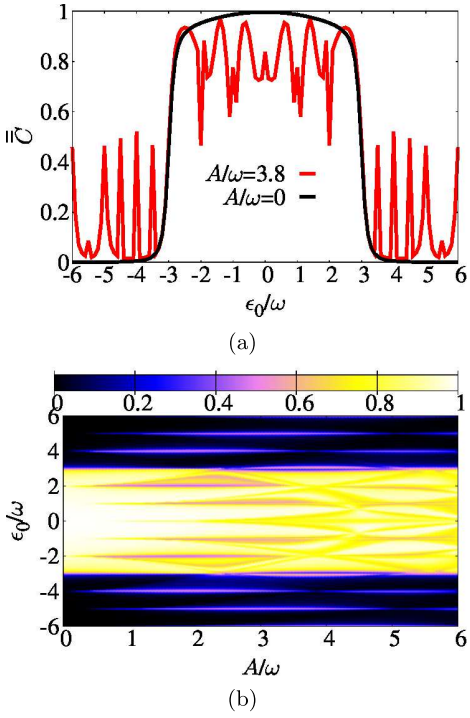

Fig. 2. (a) Plots of $\overline{\overline{C}}$ versus ϵ_0/ω for $A/\omega = 0$ (black line) and $A/\omega = 3.8$ (red line). (b) Colour map of $\overline{\overline{C}}$ versus ϵ_0/ω and A/ω. In both plots the initial condition corresponds to the ground state for the correspondent ϵ_0/ω. $J^z/\omega = -3$ is the coupling strength and other qubits parameters are the same as in Figure 1.

for $2\epsilon_0 \sim n\omega$ and $\epsilon_0 \pm J^z \sim n\omega$. They correspond to multiphoton processes where the population probability is modulated by the zeros of the Bessel functions of order n, $J_n(A/\omega) = 0$ [38,47]. Notice that while the first resonance condition gives half integer and integer values of ϵ_0/ω, the second one depends on J^z/ω. For integer values of J^z/ω the quasidegeneracies are located at integer values of ϵ_0/ω, as is clearly seen in Figure 1. However, for arbitrary J^z/ω, quasi degeneracies also appear for values of ϵ_0/ω which are neither integer nor half integers.

We will study here the cases where the system is prepared initially in the ground state and later at t_0 the ac drive is turned on. Therefore the initial state $|\Psi(t_0)\rangle$ is the ground state for the corresponding ϵ_0/ω, and we keep the same values than in Figure 1 for the other parameters. In Figure 2a we show the calculated $\overline{\overline{C}}$ as a function of ϵ_0/ω. In the absence of driving, $A/\omega = 0$ (black line), $\overline{\overline{C}}$ gives directly the concurrence of the ground state. We see that the ground state is entangled for detuning energies satisfying $|\epsilon_0/\omega| \lesssim |J^z/\omega| = 3$, where the concurrence takes values close to 1. In particular, for $\epsilon_0 = 0$, the ground state is the Bell's state $(|01\rangle + |10\rangle)/\sqrt{2}$, which is known to be a maximally entangled state [42]. On the other hand, for values $|\epsilon_0/\omega| > |J^z/\omega| = 3$ the ground state is almost disentangled, i.e. for large values of ϵ_0 the ground state is asymptotically a separable state of the computational basis, corresponding to $|00\rangle$ for $\epsilon_0 \gg 0$ and $|11\rangle$ for $\epsilon_0 \ll 0$, see Figure 1.

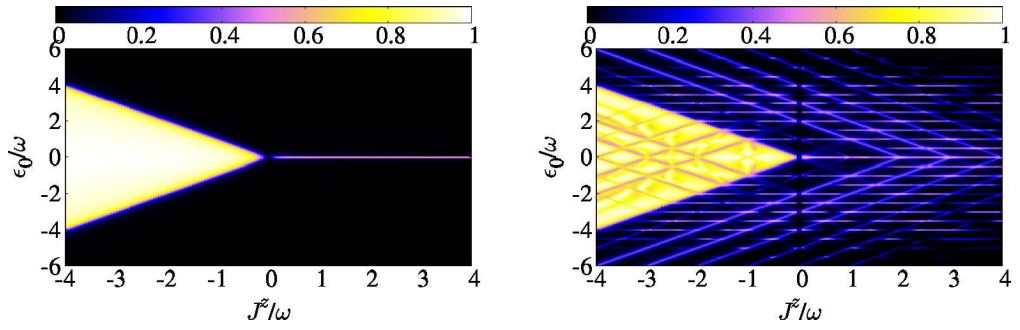

(a) $A/\omega = 0$ (b) $A/\omega = 3.8$

Fig. 3. Colour map of $\overline{\overline{C}}$ versus J^z/ω and ϵ_0/ω for $A/\omega = 0$ (a) and $A/\omega = 3.8$ (b) respectively.

When the driving is turned on ($A/\omega = 3.8$), $\overline{\overline{C}}$ displays a pattern of resonance where entanglement is either created or destroyed. For $|\epsilon_0/\omega| > |J^z/\omega| = 3$, where the initial condition corresponds to a separable state, we see that it is possible to generate entanglement in a controlled way around a given resonance. Otherwise entanglement is reduced. Notice that the positions of the resonances in $\overline{\overline{C}}$ are determined from the already mentioned conditions: $2\epsilon_0/\omega \sim n$ and $\epsilon_0/\omega + J^z/\omega \sim n$, with $n \in \mathbb{Z}$. In the present case, the resonances in Figure 2a are located at integer and half integer values of ϵ_0/ω, since $J^z/\omega = -3$. Therefore, is around a (quasi) degeneracy where the Floquet states are strongly mixed, given rise to significant deviations in the behaviour of the concurrence compared to the undriven case.

In Figure 2b we plot $\overline{\overline{C}}$ as a function of ϵ_0/ω and A/ω, for $J^z/\omega = -3$. For each particular multiphoton resonance, the concurrence is modulated by the driving amplitude, where full (or partial) recovery of the initial entanglement is possible. A related phenomenon has been already observed in single superconducting qubits, where Landau–Zener–Stuckelberg (LZS) interference patterns studied as a function of detuning ϵ_0 and amplitude A, display multiphoton resonances modulated by the coherent destruction of tunneling at certain amplitudes [32,33]. Additionally LZS interference patterns of driven coupled qubits (in the longitudinal case) have been analized [47]. In Figure 2b, we see how the LZS interference patterns show up also in the entanglement.

So far, we have studied the entanglement for a fixed value of the coupling strength. However in several practical implementations, the intensity of the coupling can be controlled. Thus it is interesting to analyze whether a different static coupling would induce qualitative changes in the above description, taking into account that the spectrum of quasienergies is sensitive to this change (see Fig. 1). In Figure 3 we plot a map of $\overline{\overline{C}}$ versus J^z/ω and ϵ_0/ω for $A/\omega = 0$ and 3.8, respectively, taking as the initial state the ground state for the corresponding ϵ_0/ω and J^z/ω.

In the absence of the microwave field (see Fig. 3a) two well separated behaviours are observed, corresponding to positive and negative values of J^z respectively. For $J^z < 0$ (antiferromagnetic coupling) the ground state is entangled for $|\epsilon_0| < |J^z|$ as we already described, given rise to the triangular shaped region in $\overline{\overline{C}}$. On the other hand, for the ferromagnetic coupling $J^z > 0$, which increases the energy of states $|01\rangle, |10\rangle$ and decreases the energy of states $|00\rangle, |11\rangle$, the ground state is entangled only for values $\epsilon_0 \sim 0$, being approximately the Bell's state $(|00\rangle + |11\rangle)/\sqrt{2}$. When the microwave field is on, $\overline{\overline{C}}$ exhibits the structure of resonances where the entanglement is created or destroyed in a well controlled way (see Fig. 3b) with resonances located at half integer or integer values of ϵ_0/ω and others located at positions determined by the values of J^z/ω, as we already mentioned. For integer values of J^z/ω the resonances are at integers ϵ_0/ω, while for arbitrary real values of J^z/ω they are respectively shifted to non integer values of ϵ_0/ω (notice the straight lines forming the >-shaped pattern).

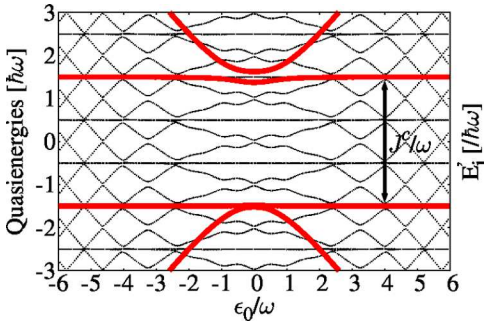

Fig. 4. Energy levels E_i' for $A/\omega = 0$ (red lines) and quasienergies for $A/\omega = 3.8$ (black lines) as a function of ϵ_0/ω for $J^c/\omega = -3$ and $p = 0$. The qubits parameters are the same as in previous figures.

We have obtained a lower bound C_I for the averaged concurrence $\overline{\overline{C}}$ (see Appendix B), that reads:

$$C_I = |\sum_{\alpha} \overline{\tilde{C}_{\alpha\alpha}(t)} \sum_{q} |a_\alpha(q)|^2| < \overline{\overline{C}}, \tag{8}$$

where $a_\alpha(q) = \langle u_\alpha(q)|\Psi(t_0)\rangle$ has been already defined and $\overline{\tilde{C}_{\alpha\alpha}(t)}$ is the time average of a *Floquet preconcurrence* $\tilde{C}_{\alpha\alpha}(t) \equiv \langle u_\alpha(t)|^* \sigma_y^{(1)} \otimes \sigma_y^{(2)} |u_\alpha(t)\rangle$. To obtain the above

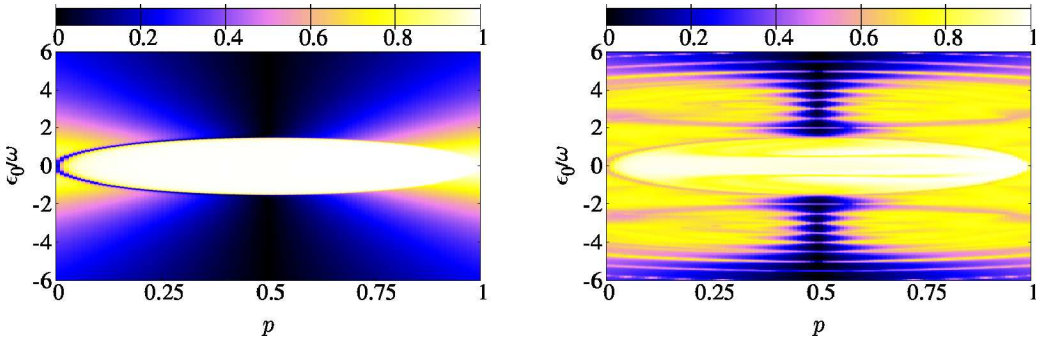

(a) $A/\omega = 0$ (b) $A/\omega = 3.8$

Fig. 5. Colour map of $\overline{\overline{C}}$ in the case of transverse coupling, as a function of ϵ_0/ω and p for $J^c/\omega = -3$.

expression for C_I we have performed a rotating wave approximation disregarding fast oscillating terms in the concurrence, so we only consider the quasienergies that fulfilled the relation $\gamma_\alpha + \gamma_\beta = n\omega$, $n \in \mathbb{Z}$. In this way C_I is mainly governed by the *Floquet preconcurrences*, each one weighted by the projection of the Floquet states on the initial condition. It should be noted that this expression is useful when the initial state is non entangled, since C_I determines the minimal creation of entanglement. For the case of weakly interacting qubits, the generation of entanglement at multiphoton resonances in the average concurrence of Floquet states, $\overline{|C_{\alpha\alpha}(t)|}$, was studied [48]. The lower bound C_I shows explicitely how the enhancement of $\overline{|C_{\alpha\alpha}(t)|}$ at the multiphoton resonances leads to an enhancement of $\overline{\overline{C}}$ in the general case. Since Floquet states are not accessible experimentally, one has to consider the full expression equation (8) in general situations. Furthermore, our results apply beyond the weak interaction case.

3.2 Transverse coupling

In this section we focus on the "transverse coupling" case $J^z = 0$, $J^c \neq 0$, for which $[V(t), \hat{H}_{12}] \propto J^c(1-2p)$.

Figure 4 shows the eigenenergies E'_i, $i = 0, \ldots, 3$, as a function of ϵ_0/ω for the static Hamiltonian for $J^c/\omega = -3$ and $p = 0$. For $p = 0$ the coupling Hamiltonian is $\hat{H}^c_{12} = -J^c/2\sigma_x^{(1)}\sigma_x^{(2)}$. In this case the coupling breaks the degeneracy between $|01\rangle, |10\rangle$ but also mixes the states $|00\rangle$ and $|11\rangle$, given rise to the exhibited spectrum. Additionally we plot the quasienergies for the driven Hamiltonian in black lines, for the amplitude $A/\omega = 3.8$.

For the $p = 0$ case under consideration, we get the analytical expressions $\gamma_\alpha \sim \pm\sqrt{\epsilon_0^2 + (J_c/2)^2} + m\omega$ and $\pm J^c/2 + m\omega$ for the quasienergies, assuming $\Delta_i/\omega \to 0$ and $A/\omega \to 0$. Thus, the resonance conditions are fulfilled for $J^c/\omega \sim n$ (independent of the detuning), for values satisfying $(2\epsilon_0/\omega)^2 + (J^c/\omega)^2 \sim n^2$ and for $J^c/2\omega \pm \sqrt{(\epsilon_0/\omega)^2 + (J^c/2\omega)^2} \sim n$. The two latter conditions give rise to an intricate pattern of quasidegeneracies in the spectrum of Figure 4, that will induce a non trivial behaviour in the concurrence, as we show below.

It is interesting to analyze the dependence of $\overline{\overline{C}}$ on ϵ_0/ω and on p. Notice that by changing p, one get different values of the commutator $[V(t), \hat{H}_{12}] \propto J^c(1-2p)$. (Additionally, in experimental implementations it could be possible to control the magnitude of $[V(t), \hat{H}_{12}]$ by driving the qubits with different amplitudes A instead of changing p, see equation (6)). Figure 5a shows the results without driving for $J^c/\omega = -3$. Two well defined regions exhibiting a qualitative change in the behavior of the concurrence of the ground state are observed. For $0 < p < 0.5$ the coupling $J^c/2\sigma_x^{(1)} \otimes \sigma_x^{(2)}$ is the dominant term in the Hamiltonian $\hat{H}_{12}$. In this case, for $\epsilon_0 \sim 0$ the ground state is separable corresponding to the singlet states $|s_1\rangle|s_2\rangle$, but as p increases it also does the term $J^c/2\sigma_y^{(1)}\sigma_y^{(2)}$, and the ground state becomes entangled. For the region $0.5 < p < 1$ the dominant term is $J^c/2\sigma_y^{(1)} \otimes \sigma_y^{(2)}$ and in this case the ground state remains maximally entangled near $\epsilon_0 \sim 0$ as p decreases. In Figure 5b we present the results for driving amplitude $A/\omega = 3.8$. For $p = 0.5$ the commutator vanishes and the entanglement resonances are well defined. When departing from $p = 0.5$, the resonances start to spread as a function of $|1-2p|$. An important creation of entanglement, with a rich (and non trivial) pattern of wide resonances, is clearly observed in an ample range of $p \neq 0.5$. In the extreme case of $p = 0$ (and similarly for $p = 1$) the entanglement is created in a broad range of ϵ_0/ω, specially near $\epsilon_0 = 0$, where the initial state is a separable state (corresponding to a singlet state). For larger values of ϵ_0/ω we observe in both cases a quite similar pattern, with the creation of entanglement due to the driving, but with wider and overlapping resonances compared to the $p = 0.5$ case. This behavior is concomitant with the landscape of avoided crossings in the quasienergies spectrum, as a consequence of the non commutation of the static Hamiltonian with the driving field. The wide resonances generate a region where entanglement is quite robust to changes in the detuning. This could be a tool to stabilize the entanglement created by the driving field.

Besides changing the dominant interaction in the coupling Hamiltonian, one can analyze the sensitivity of the concurrence with the coupling strength for a fix value of p. As an example we focus on the $p = 0$ case. The pattern displayed in Figure 6a in the absence of driving is consistent with the resonant conditions obtained previously for $(\Delta_i, A) \to 0$. In particular notice the regions

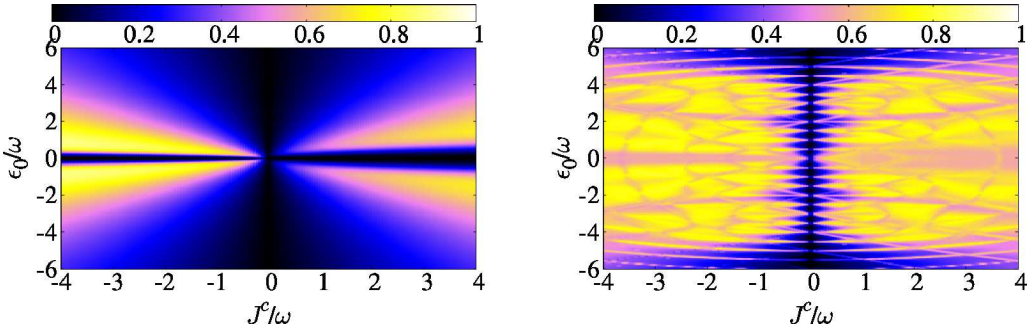

(a) $A/\omega = 0$ (b) $A/\omega = 3.8$

Fig. 6. Colour map of $\overline{\overline{C}}$ versus J^c/ω and ϵ_0/ω for transverse coupling with $p = 0$.

where the quasi linear behaviour with J^c/ω dominates for $\epsilon_0/\omega \sim 0$, turning into parabolic ones in the plane $(\epsilon_0/\omega, J^c/\omega)$, for larger values of detuning. The concurrence takes different values along these regions, even for a fixed J^c/ω. When the driving is turned on, for weak coupling $J^c \sim 0$, we see well defined resonances in $\overline{\overline{C}}$. However, when $|J^c/\omega| \gtrsim 1$ the driving induces a drastic change in this behaviour. Unlike the longitudinal coupling, or the weak transverse coupling, where the behavior with J^c/ω for finite driving was quite predictable, we observe non trivial features in the strong transverse coupling case. Among others, is the generation of an important amount of *homogeneous* entanglement for a wide range of detuning and static coupling strength. Additionally the concurrence exhibits a quite symmetric pattern for $J^c/\omega \lessgtr 0$.

4 Conclusions

In this work we have shown that entanglement can be manipulated by external periodic driving fields. In particular we presented extensive numerical and analytical results for the concurrence of a system composed by two coupled qubits driven by an external ac magnetic flux, neglecting the effect of dissipation. Our results apply to the case of highly coherent qubits [49], when the driving is on for time scales smaller than the decoherence time T_2 and such that $\omega T_2 \gg 1$. For time scales $t < T_2$ the entanglement generated will be stable. Currently, superconducting qubits are fabricated with decoherence times as large as $T_2 \sim 100\,\mu$s [49] and therefore the entanglement generated by the ac drive can be maintained coherently for several driving periods for typical rf frequencies. The average concurrence $\overline{\overline{C}}$ defined in equation (6) has been used here as a theoretical tool to characterize the typical expected degree of entanglement in a time dependent state. Of course, this quantity as given in the mathematical expression of equation (6), is not directly accessible in the experiment. The concurrence $C(t)$ can be measured in superconducting qubits by quatum state tomography for a finite time interval [44]. The generation of entanglement described here will be shown in this type of protocols as a difference in the measured $C(t)$ with and without the applied ac drive.

Under the above mentioned condition, $\omega T_2 \gg 1$, there are different behaviours in the concurrence, depending on the commutability of the driving term with the qubit–qubit interaction term. In the special cases when the driving term and the interaction term in the Hamiltonian commute (longitudinal coupling), the control of entanglement is almost complete within a narrow range of the multiphoton resonances. The advantage of this scenario is that (a) when the initial state is disentangled, it can be driven towards a highly entangled state, and (b) when the initial state is entangled, one can strongly reduce entanglement with the driving.

In view of entanglement manipulation, our more important result is for the transverse coupling between the qubits, when the driving Hamiltonian and the interaction Hamiltonian do not commute. In this case, we find that the multiphoton resonances in the concurrence, as seen in terms of an entanglement measure, are spread and overlap. In the $\{\epsilon_0, J^c\}$ plane in Figure 6b this shows as broad regions where entanglement can be enhanced starting from a disentangled initial condition, even away from a resonance. Therefore the control of entanglement is robust in parameter space, being a more convenient situation for practical implementations of driving induced entanglement.

We acknowledge support from CNEA, CONICET, UNCuyo (P 06/C455) and ANPCyT (PICT2014-1382).

Author contribution statement

All the authors were involved in the preparation of the manuscript. All the authors have read and approved the final manuscript.

Appendix A: Calculation of concurrence in Floquet basis

We calculate the concurrence $C(t, t_0) = |\langle\Psi(t)|^* |\sigma_y^{(1)} \otimes \sigma_y^{(2)}|\Psi(t)\rangle|$ [42] using the expansion of $|\Psi(t)\rangle$ in the Floquet

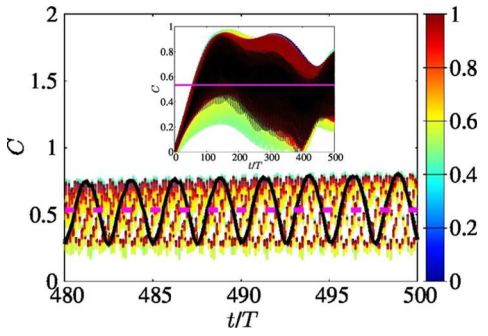

Fig. A.1. Plots of the concurrence $C(t,t_0)$ for $\epsilon_0/\omega = 4$ and $A/\omega = 3.8$, as a function of the normalized time t/T for 300 different initial times t_0/T, represented on the vertical colour bar. The initial state is $|\Psi(t_0)\rangle$. In black line $\overline{C(t)}$ is plotted and in dashed magenta, its average $\overline{\overline{C}}$. The inset show the plot in the range $t/T \in [0, 500]$, while the main figure shows a detail in the interval $t/T \in [480, 500]$. Results correspond to longitudinal coupling with $J^z/\omega = -3$. Parameters are $\Delta_1/\omega = 0.1$ and $\Delta_2/\omega = 0.15$.

basis [35]:

$$C(t,t_0) = |\sum_{\alpha\beta} a_\alpha(t_0)a_\beta(t_0) \times e^{-i(\gamma_\alpha+\gamma_\beta)(t-t_0)}\tilde{C}_{\alpha\beta}(t)|, \quad (A.1)$$

with $a^\alpha_\beta(t_0) = \langle u^\alpha_\beta(t_0)|\Psi(t_0)\rangle$, $|u^\alpha_\beta(t)\rangle$ the Floquet states and γ^α_β the quasienergies. The initial condition is $|\Psi(t_0)\rangle$ and $\tilde{C}_{\alpha\beta}(t) = \langle u_\alpha(t)|^* \sigma_y \otimes \sigma_y |u_\beta(t)\rangle$.

Employing the extended Fourier basis $|u_\alpha(t)\rangle = \sum_k e^{-ik\omega t}|u_\alpha(k)\rangle$ and $\langle u_\alpha(t_0)| = \sum_q e^{iq\omega t}\langle u_\alpha(q)|$, the equation (A.1) reads

$$C(t,t_0) = |\sum_{\alpha\beta kk'qq'} \tilde{C}_{\alpha\beta}(k,k')f_{\alpha\beta}(q,q') \times e^{-i\varphi^{kk'qq'}_{\alpha\beta}(t,t_0)}|, \quad (A.2)$$

where $\varphi^{kk'qq'}_{\alpha\beta}(t,t_0) = (\gamma_\beta + \gamma_\alpha - (k'+k)\omega)t - (\gamma_\beta + \gamma_\alpha - (q'+q)\omega)t_0$, $\tilde{C}_{\alpha\beta}(k,k') = \langle u_\alpha(k)|^* \sigma_y \otimes \sigma_y |u_\beta(k')\rangle$ and $f_{\alpha\beta}(q,q') = a_\alpha(q)a_\beta(q')$, with $a^\alpha_\beta(^q_{q'}) = \langle u^\alpha_\beta(^q_{q'})|\Psi(t_0)\rangle$.

Under general conditions, the initial time should be averaged out, thus we compute the time-averaged concurrence over t_0,

$$\overline{C(t)} = \frac{1}{T}\int_0^T dt_0\, C(t,t_0),$$

with $T = 2\pi/\omega$ the driving period. It is useful to characterize the typical concurrence of a time dependent system with an aditional average

$$\overline{\overline{C}} = \lim_{T\to\infty}\frac{1}{T}\int_0^T dt\, \overline{C(t)}.$$

Figure A.1 displays the concurrence $C(t,t_0)$ as a function of the normalized time t/T calculated for the initial condition $|\Psi(t_0)\rangle = e^{-iE_0t_0}|E_0\rangle$, which was chosen as the ground state of the time independent Hamiltonian (with eigenvalue E_0) for detuning energy $\epsilon_0/\omega = 4$ and static coupling strength $J^z/\omega = -3$, corresponding to the longitudinal coupling case. The driving amplitude chosen is $A/\omega = 3.8$. $C(t,t_0)$ was computed for around 300 different initial times with $t_0/T \in [0,1]$. Notice that due to the different initial times, that induce a different initial phase in the microwave field, the curves are shifted. After averaging over t_0, $\overline{C}(t)$, turns out to be a smoother function whose time average $\overline{\overline{C}}$, results independent on time as expected.

Appendix B: Lower bound for time-averaged concurrence

Here we calculate a lower bound for $\overline{\overline{C}}$, the averaged concurrence over (t,t_0). First we expand the equation (A.2) as

$$C(t,t_0) = |\sum_{\alpha\beta kk'qq'} \tilde{C}_{\alpha\beta}(k,k')f_{\alpha\beta}(q,q')\cos(\varphi^{kk'qq'}_{\alpha\beta}(t,t_0) + i\sum_{\alpha\beta kk'qq'} \tilde{C}_{\alpha\beta}(k,k')f_{\alpha\beta}(q,q') \times \sin(\varphi^{kk'qq'}_{\alpha\beta}(t,t_0))|, \quad (B.1)$$

where we separate the real (Re) and imaginarie (Im) part. Using the relations $|z| \geq |Re(z)|, |Im(z)|$ for a complex number $z \in \mathbb{C}$, from equation (B.1) we get

$$C(t,t_0) \geq |\sum_{\alpha\beta kk'qq'} \tilde{C}_{\alpha\beta}(k,k')f_{\alpha\beta}(q,q')\cos(\varphi^{kk'qq'}_{\alpha\beta}(t,t_0)|,$$
$$C(t,t_0) \geq |\sum_{\alpha\beta kk'qq'} \tilde{C}_{\alpha\beta}(k,k')f_{\alpha\beta}(q,q')\sin(\varphi^{kk'qq'}_{\alpha\beta}(t,t_0))|. \quad (B.2)$$

Now we apply the inequality $\int_a^b |f(x)|dx \geq |\int_a^b f(x)dx|$, with $f(x) : \mathbb{R} \to \mathbb{R}$ and $a < b$, to equation (B.2). After defining the lower bound limit as $\overline{\overline{C}} = \frac{1}{T}\int_0^T dt \frac{1}{T}\int_0^T dt_0 C(t,t_0)$, we obtain for equation (B.2) two lower bounds C_I and C_{II}:

$$C_I = |\sum_{\alpha\beta kk'qq'} \tilde{C}_{\alpha\beta}(k,k')f_{\alpha\beta}(q,q')\overline{\overline{\cos(\varphi^{kk'qq'}_{\alpha\beta}(t,t_0)}}|,$$
$$C_{II} = |\sum_{\alpha\beta kk'qq'} \tilde{C}_{\alpha\beta}(k,k')f_{\alpha\beta}(q,q')\overline{\overline{\sin(\varphi^{kk'qq'}_{\alpha\beta}(t,t_0))}}|, \quad (B.3)$$

satisfying $\overline{\overline{C}} \geq C_I, C_{II}$.

Using the trigonometric identities $\sin(A-B) = \sin(A)\cos(B) - \cos(A)\sin(B)$ and $\cos(A-B) = \cos(A)\cos(B) + \sin(A)\sin(B)$, and taking the average

over (t, t_0) we obtain

$$\begin{aligned}\overline{\overline{\cos(\varphi_{\alpha\beta}^{kk'qq'}(t,t_0))}} &= \delta_{\gamma_\alpha+\gamma_\beta-n\omega,0}\,\delta_{\gamma_\alpha+\gamma_\beta-m\omega,0} \\ &\quad+\delta_{\gamma_\alpha+\gamma_\beta-n\omega,\pi/(2T)}\,\delta_{\gamma_\alpha+\gamma_\beta-m\omega,\pi/(2T)}, \\ \overline{\overline{\sin(\varphi_{\alpha\beta}^{kk'qq'}(t,t_0))}} &= \delta_{\gamma_\alpha+\gamma_\beta-n\omega,\pi/(2T)}\,\delta_{\gamma_\alpha+\gamma_\beta-m\omega,0} \\ &\quad-\delta_{\gamma_\alpha+\gamma_\beta-n\omega,0}\,\delta_{\gamma_\alpha+\gamma_\beta-m\omega,\pi/(2T)},\end{aligned} \tag{B.4}$$

with $n = k + k'$ and $m = q + q'$. Replacing $T = 2\pi/\omega$ and ordering the terms, we get

$$\begin{aligned}\overline{\overline{\cos(\varphi_{\alpha\beta}^{kk'qq'}(t,t_0))}} &= \delta_{\gamma_\alpha+\gamma_\beta,n\omega}\,\delta_{\gamma_\alpha+\gamma_\beta,m\omega} \\ &\quad+\delta_{\gamma_\alpha+\gamma_\beta,(n+1/4)\omega}\,\delta_{\gamma_\alpha+\gamma_\beta,(m+1/4)\omega}, \\ \overline{\overline{\sin(\varphi_{\alpha\beta}^{kk'qq'}(t,t_0))}} &= \delta_{\gamma_\alpha+\gamma_\beta,(n+1/4)\omega}\,\delta_{\gamma_\alpha+\gamma_\beta,m\omega} \\ &\quad-\delta_{\gamma_\alpha+\gamma_\beta,n\omega}\,\delta_{\gamma_\alpha+\gamma_\beta,(m+1/4)\omega}.\end{aligned} \tag{B.5}$$

We assume that the main contribution to the concurrence is near the resonances condition $\gamma_\alpha + \gamma_\beta = n\omega$, which is equivalent to a rotating wave approximation disregarding fast oscillating terms. Thus

$$\begin{aligned}\overline{\overline{\cos(\varphi_{\alpha\beta}^{kk'qq'}(t,t_0))}} &\sim \delta_{\gamma_\alpha+\gamma_\beta,n\omega}\,\delta_{\gamma_\alpha+\gamma_\beta,m\omega}, \\ \overline{\overline{\sin(\varphi_{\alpha\beta}^{kk'qq'}(t,t_0))}} &\sim 0.\end{aligned} \tag{B.6}$$

Using the last result we obtain $C_I \geq C_{II} = 0$, then the corresponding lower bound expression is

$$\begin{aligned}C_I \sim |\sum_{\substack{\alpha\beta\\knqm}} &\tilde{C}_{\alpha\beta}(k,n-k) f_{\alpha\beta}(q,m-q) \\ &\times\delta_{\gamma_\alpha+\gamma_\beta,n\omega}\,\delta_{\gamma_\alpha+\gamma_\beta,m\omega}|.\end{aligned} \tag{B.7}$$

Given equation (B.7), we employ the condition $\gamma_\beta = -\gamma_\alpha + n\omega$ on the Floquet quasienergies, obtaining

$$\begin{aligned}e^{-i\gamma_\beta}|u_\beta(t)\rangle &= e^{i\gamma_\alpha}e^{-in\omega}|u_\beta(t)\rangle, \\ &= e^{i\gamma_\alpha}e^{-in\omega}\sum_k e^{ik\omega t}|u_\beta(k)\rangle \\ &= e^{i\gamma_\alpha}\sum_k e^{i(k-n)\omega t}|u_\beta(k)\rangle \\ &= e^{i\gamma_\alpha}\sum_k e^{ik\omega t}|u_\beta(k-n)\rangle \\ &= e^{i\gamma_\alpha}\sum_k e^{-ik\omega t}|u_\beta(n-k)\rangle.\end{aligned} \tag{B.8}$$

It is straightforward show that

$$\begin{aligned}(e^{-i\gamma_\alpha}|u_\alpha(t)\rangle)^* &= e^{i\gamma_\alpha}|u_\alpha(t)\rangle^*, \\ &= e^{i\gamma_\alpha}\sum_k e^{-ik\omega t}|u_\alpha(k)\rangle^* \\ &= e^{i\gamma_\alpha}\sum_k e^{-ik\omega t}|u_\alpha(-k)\rangle.\end{aligned} \tag{B.9}$$

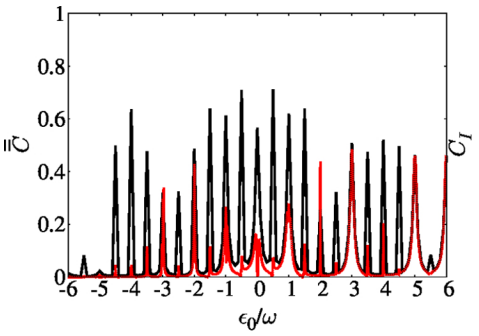

Fig. B.1. Plot of $\overline{\overline{C}}$ (black line) and C_I (red line) as a function of ϵ_0/ω. With $A/\omega = 3.8$ and the coupling strength $J^z/\omega = -3$. The other qubits parameters are the same than in Figure 1.

Then, from equations (B.8) and (B.9), the equivalence relation is satisfied:

$$\gamma_\beta \to -\gamma_\alpha + n\omega \Rightarrow |u_\beta(n-k)\rangle \to |u_\alpha(-k)\rangle. \tag{B.10}$$

Using the equation (B.10) with $n = k + k'$ and $m = q + q'$, the lower bound in equation (B.7) reads

$$C_I \sim |\sum_{\alpha kq} \tilde{C}_{\alpha\alpha}(k,-k) f_{\alpha\alpha}(q,-q)|. \tag{B.11}$$

From which we identify a contribution of the form

$$\sum_k \tilde{C}_{\alpha\alpha}(k,-k) = \frac{1}{T}\int_0^T dt\, \tilde{C}_{\alpha\alpha}(t) = \overline{\tilde{C}_{\alpha\alpha}(t)}, \tag{B.12}$$

where $\tilde{C}_{\alpha\alpha}(t) = \langle u_\alpha(t)|^* \sigma_y \otimes \sigma_y |u_\alpha(t)\rangle$ is the *Floquet pre-concurrence*. Also, using $|u_\alpha(-q)\rangle = |u_\alpha(q)\rangle^*$ we obtain that

$$\begin{aligned}f_{\alpha\alpha}(-q,q) &= a_\alpha(-q)a_\alpha(q) = a_\alpha^*(q)a_\alpha(q) \\ &= |a_\alpha(q)|^2,\end{aligned} \tag{B.13}$$

corresponding to the amplitude of the Floquet states projections over the initial condition.

Finally replacing equations (B.12) and (B.13) in equation (B.11) we obtain

$$C_I \sim |\sum_\alpha \overline{\tilde{C}_{\alpha\alpha}(t)} \sum_q |a_\alpha(q)|^2|. \tag{B.14}$$

This expression is useful for the non-entangled initial state since it represents the minimal entanglement creation.

In Figure B.1 we plot $\overline{\overline{C}}$ and C_I for the longitudinal coupling case, both as a function of ϵ_0/ω. We choose the initial state $|00\rangle$, corresponding to a separable state (of the computational basis), and work with the driven amplitude $A/\omega = 3.8$. The coupling strength is $J^z/\omega = -3$. The position of the resonances at integer values of ϵ_0/ω are well captured by the lower bound C_I, and the agreement with $\overline{\overline{C}}$ is quite good. Notice however that for half integer values

of ϵ_0/ω, $\overline{\overline{C}}$ also exhibits resonances that are quite attenuated in C_I. This behaviour can be understood taking into account that the stationary phase condition employed to compute C_I involves the sum $\gamma_\alpha + \gamma_\beta$ of pairs of quasienergies, which gives either ϵ_0 or J^z. Therefore for integer values of J^z/ω and ϵ_0/ω, the resonance conditions and the stationary phase condition are both satisfied. On the other hand, for half integer values of ϵ_0/ω the stationary phase approximation is not fulfilled, and the resonances displayed in $\overline{\overline{C}}$ are dimmed in C_I.

References

1. I. Bloch, Nature **453**, 1016 (2008)
2. H. Krauter, C.A. Muschik, K. Jensen, W. Wasilewski, J.M. Petersen, J.I. Cirac, E.S. Polzik, Phys. Rev. Lett. **107**, 080503 (2011)
3. R. Blatt, D. Wineland, Nature **453**, 1008 (2008)
4. J.T. Barreiro, M. Muller, P. Schindler, D. Nigg, T. Monz, M. Chwalla, M. Hennrich, C.F. Roos, P. Zoller, R. Blatt, Nature **470**, 486 (2011)
5. C. Rigetti, M. Devoret, Phys. Rev. B **81**, 134507 (2010)
6. S. Poletto, J.M. Gambetta, S.T. Merkel, J.A. Smolin, J.M. Chow, A.D. Córcoles, G.A. Keefe, M.B. Rothwell, J.R. Rozen, D.W. Abraham et al., Phys. Rev. Lett. **109**, 240505 (2012)
7. Z.H. Peng, Y.X. Liu, Y. Nakamura, J.S. Tsai, Phys. Rev. B **85**, 024537 (2012)
8. J.M. Chow, L. DiCarlo, J.M. Gambetta, A. Nunnenkamp, L.S. Bishop, L. Frunzio, M.H. Devoret, S.M. Girvin, R.J. Schoelkopf, Phys. Rev. A **81**, 062325 (2010)
9. T.P. Orlando, J.E. Mooij, L. Tian, C.H. van der Wal, L.S. Levitov, S. Lloyd, J.J. Mazo, Phys. Rev. B **60**, 15398 (1999)
10. J.R. Friedman, V. Patel, W. Chen, S.K. Tolpygo, J.E. Lukens, Nature **406**, 43 (2000)
11. C.H. van der Wal, A.C.J. ter Haar, F.K. Wilhelm, R.N. Schouten, C.J.P.M. Harmans, T.P. Orlando, S. Lloyd, J.E. Mooij, Science **290**, 773 (2000)
12. J.M. Martinis, S. Nam, J. Aumentado, C. Urbina, Phys. Rev. Lett. **89**, 117901 (2002)
13. G. Wendin, V.S. Shumeiko, Low Temp. Phys. **33**, 724 (2007)
14. J. Clarke, F.K. Wilhelm, Nature **453**, 1031 (2008)
15. A. Izmalkov, M. Grajcar, E. Il'ichev, T. Wagner, H.G. Meyer, A.Y. Smirnov, M.H.S. Amin, A.M. van den Brink, A.M. Zagoskin, Phys. Rev. Lett. **93**, 037003 (2004)
16. M. Grajcar, A. Izmalkov, S.H.W. van der Ploeg, S. Linzen, E. Il'ichev, T. Wagner, U. Hübner, H.G. Meyer, A. Maassen van den Brink, S. Uchaikin et al., Phys. Rev. B **72**, 020503 (2005)
17. J.B. Majer, F.G. Paauw, A.C.J. ter Haar, C.J.P.M. Harmans, J.E. Mooij, Phys. Rev. Lett. **94**, 090501 (2005)
18. T. Yamamoto, Y.A. Pashkin, O. Astafiev, Y. Nakamura, J.S. Tsai, Nature **425**, 941 (2003)
19. F.W. Strauch, P.R. Johnson, A.J. Dragt, C.J. Lobb, J.R. Anderson, F.C. Wellstood, Phys. Rev. Lett. **91**, 167005 (2003)
20. J.E. Mooij, T.P. Orlando, L. Levitov, L. Tian, C.H. van der Wal, S. Lloyd, Science **285**, 1036 (1999)
21. S.H.W. van der Ploeg, A. Izmalkov, A.M. van den Brink, U. Hübner, M. Grajcar, E. Il'ichev, H.G. Meyer, A.M. Zagoskin, Phys. Rev. Lett. **98**, 057004 (2007)
22. B.L.T. Plourde, J. Zhang, K.B. Whaley, F.K. Wilhelm, T.L. Robertson, T. Hime, S. Linzen, P.A. Reichardt, C.E. Wu, J. Clarke, Phys. Rev. B **70**, 140501 (2004)
23. K. Harrabi, F. Yoshihara, A.O. Niskanen, Y. Nakamura, J.S. Tsai, Phys. Rev. B **79**, 020507 (2009)
24. P.C. de Groot, J. Lisenfeld, R.N. Schouten, S. Ashhab, A. Lupascu, C.J.P.M. Harmans, J.E. Mooij, Nat. Phys. **6**, 763 (2010)
25. Y. Nakamura, Y.A. Pashkin, J.S. Tsai, Phys. Rev. Lett. **87**, 246601 (2001)
26. S. Shevchenko, S. Ashhab, F. Nori, Phys. Rep. **492**, 1 (2010)
27. D.M. Berns, W.D. Oliver, S.O. Valenzuela, A.V. Shytov, K.K. Berggren, L.S. Levitov, T.P. Orlando, Phys. Rev. Lett. **97**, 150502 (2006)
28. M.S. Rudner, A.V. Shytov, L.S. Levitov, D.M. Berns, W.D. Oliver, S.O. Valenzuela, T.P. Orlando, Phys. Rev. Lett. **101**, 190502 (2008)
29. A. Izmalkov, S.H.W. van der Ploeg, S.N. Shevchenko, M. Grajcar, E. Il'ichev, U. Hübner, A.N. Omelyanchouk, H.G. Meyer, Phys. Rev. Lett. **101**, 017003 (2008)
30. C. Deng, J.L. Orgiazzi, F. Shen, S. Ashhab, A. Lupascu, Phys. Rev. Lett. **115**, 133601 (2015)
31. P. Neilinger, S.N. Shevchenko, J. Bogár, M. Rehák, G. Oelsner, D.S. Karpov, U. Hübner, O. Astafiev, M. Grajcar, E. Il'ichev, Phys. Rev. B **94**, 094519 (2016)
32. W.D. Oliver, Y. Yu, J.C. Lee, K.K. Berggren, L.S. Levitov, T.P. Orlando, Science **310**, 1653 (2005)
33. W.D. Oliver, S.O. Valenzuela, Quant. Inf. Process. **8**, 261 (2009)
34. A. Ferrón, D. Domínguez, M.J. Sánchez, Phys. Rev. B **82**, 134522 (2010)
35. J.H. Shirley, Phys. Rev. **138**, B979 (1965)
36. A. Ferrón, D. Domínguez, M.J. Sánchez, Phys. Rev. Lett. **109**, 237005 (2012)
37. A. Ferrón, D. Domínguez, M.J. Sánchez, Phys. Rev. B **93**, 064521 (2016)
38. S.K. Son, S. Han, S.I. Chu, Phys. Rev. A **79**, 032301 (2009)
39. J. Hausinger, M. Grifoni, Phys. Rev. A **81**, 022117 (2010)
40. S. Ashhab, J.R. Johansson, A.M. Zagoskin, F. Nori, Phys. Rev. A **75**, 063414 (2007)
41. A. Dewes, F.R. Ong, V. Schmitt, R. Lauro, N. Boulant, P. Bertet, D. Vion, D. Esteve, Phys. Rev. Lett. **108**, 057002 (2012)
42. W.K. Wootters, Phys. Rev. Lett. **80**, 2245 (1998)
43. M.D. Shulman, O.E. Dial, S.P. Harvey, H. Bluhm, V. Umansky, A. Yacoby, Science **336**, 202 (2012)
44. N. Roch, M.E. Schwartz, F. Motzoi, C. Macklin, R. Vijay, A.W. Eddins, A.N. Korotkov, K.B. Whaley, M. Sarovar, I. Siddiqi, Phys. Rev. Lett. **112**, 170501 (2014)
45. A. Narla, S. Shankar, M. Hatridge, Z. Leghtas, K.M. Sliwa, E. Zalys-Geller, S.O. Mundhada, W. Pfaff, L. Frunzio, R.J. Schoelkopf et al., Phys. Rev. X **6**, 031036 (2016)
46. G. Romero, C.E. López, F. Lastra, E. Solano, J.C. Retamal, Phys. Rev. A **75**, 032303 (2007)

47. A.M. Satanin, M.V. Denisenko, S. Ashhab, F. Nori, Phys. Rev. B **85**, 184524 (2012)
48. S. Sauer, F. Mintert, C. Gneiting, A. Buchleitner, J. Phys. B: At. Mol. Opt. Phys. **45**, 154011 (2012)
49. F. Yan, S. Gustavsson, A. Kamal, J. Birenbaum, A.P. Sears, D. Hover, T.J. Gudmundsen, D. Rosenberg, G. Samach, S. Weber et al., Nat. Commun. **7**, 12964 (2016)